

Measurement of the Potassium 4P Excited State Diffusion Coefficient in Xenon Gas Using Degenerate Four-Wave Mixing

D. S. Glassner and R. J. Knize

Department of Physics and Astronomy, University of Southern California, Los Angeles, California 90089-0484

(Received 7 October 1994)

We present a method for measuring the diffusion coefficients for excited atoms in buffer gases that uses degenerate four-wave mixing. We show that, for low beam intensities and atomic densities, the relative angular response of the degenerate four-wave mixing signal is dependent on the excited state diffusion and decay rate only, and that it is independent of the ground state diffusion. We have experimentally measured the diffusion of potassium atoms in the 4P state in xenon and found that the diffusion coefficient D at 155 °C and 760 torr is $0.084(4) \text{ cm}^2 \text{ s}^{-1}$.

PACS numbers: 42.65.Hw, 34.50.-s, 39.30.+w

The diffusion of atoms and molecules in a gas is a fundamental transport phenomenon. Almost all previous experiments have measured ground state diffusion [1]. Recently, the diffusion of excited alkali atoms in inert buffer gases has received much attention. This interest has been driven by effects based on the fact that an excited atom can exhibit a different diffusion cross section as compared to a ground state atom. This difference between the diffusion cross sections results in the effects of light-induced drift [2,3] and light diffusive pulling [4,5]. A related phenomenon known as white-light-induced drift is thought to explain the abundance anomalies of some isotopes in certain stellar bodies [6]. Excited state diffusion is also of interest for performing isotope separation [7], as well as testing intermolecular scattering potentials [8]. Previous measurements of the diffusion of short-lived excited states have examined the light transmission of a probe beam with and without an overlapping, strong pump beam. From the ratio of these two measurements, the relative change of the diffusion cross section between the ground and excited states is calculated. In this Letter we present a new method for measuring the excited state diffusion coefficients. We show that the dependence of a degenerate four-wave mixing signal on the angle between the two forward beams allows a direct determination of the excited state diffusion coefficient independent of the ground state coefficient. This method does not depend on any higher order diffusion modes or on time-dependent behavior.

Degenerate four-wave mixing (DFWM) is the result of two beams writing an interference grating in a nonlinear medium, which then allows a third beam to scatter, creating a fourth beam, as shown schematically in Fig. 1(a). Most theoretical treatments for DFWM in atomic vapors approximate the interaction as two-level atoms interacting with monochromatic laser fields. For stationary, two-level atoms, it is possible to compute a complete solution for the generated wave for arbitrary input beam intensities [9]. However, for real atomic vapors, which have thermal motion, a general solution is not possible, and models

using third order perturbation theory for low intensities have been developed [10–12]. These models assume that the atoms possess a Maxwellian velocity distribution and do not have velocity changing collisions within the time scale of interest, i.e., the excited state lifetime. Under these conditions, the atoms can move across the intensity gratings the input beams create, and for short grating spacings the DFWM effect is “washed out.” These predictions have been confirmed by experiments [13] and have shown that the DFWM signal decreases rapidly as the angle θ between the forward beams exceeds $\Theta_0 \approx 5\text{--}10 \text{ mrad}$ for most alkali atoms at the temperatures

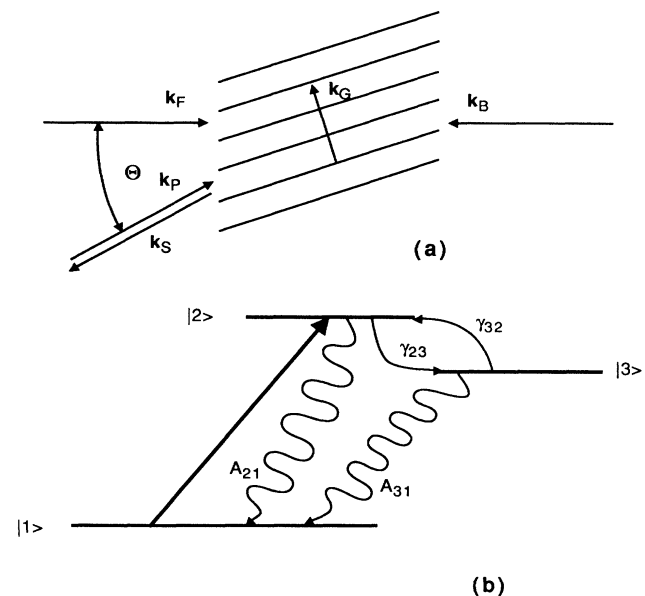


FIG. 1. (a) Diagram showing the grating written by the forward pump and probe beams and the signal beam that result when the backward pump scatters from the grating. (b) Simple level scheme showing ground, resonant excited state and nonresonant, collisionally mixed excited state. Solid straight arrow represents optical excitation, wiggly arrows represent radiative decay, and curved arrows represent collisional mixing.

typically utilized. Even homogeneously broadened atomic vapors exhibit an angular dependence in the four-wave mixing signal due to the motion of the atoms. However, at large buffer gas densities, the atoms can experience many velocity-randomizing collisions while in the excited state. The atoms will not be able to move freely across the intensity gratings, and the washing out of the population gratings will be reduced. In this case the models mentioned above will need to be modified to account for the diffusive movement of the atoms.

When the time between collisions becomes much less than the excited state lifetime, the density matrix can be described by a modified, quantum mechanical transport equation [10],

$$i\hbar\left(\frac{\partial}{\partial t} - D\nabla^2\right)\hat{\rho} = [\hat{H}_0, \hat{\rho}] + [\hat{V}, \hat{\rho}] + \text{relaxation terms}, \quad (1)$$

where $\hat{\rho}$ is the density matrix, D represents an operator that describes diffusion, \hat{H}_0 is the atomic Hamiltonian, \hat{V} accounts for the applied fields, and the "relaxation terms" include spontaneous emission and dephasing collisions. The density matrix can be determined from Eq. (1) by using a perturbation expansion in powers of the applied electric fields. For fields below the saturation intensity and in the steady state, we find that the nonlinear polarization that generates the DFWM signal is proportional to the population difference between the ground and excited states, labeled "1" and "2," respectively, as shown in Fig. 1(b). This population difference can be written as

$$\rho_2^{(2)} - \rho_1^{(2)} \propto \frac{1}{A_{21} + D_2 k_G^2} \left\{ 1 + \frac{D_2}{D_1} \right\}, \quad (2)$$

where $\rho_2^{(2)} - \rho_1^{(2)}$ is the population difference with the correct phase and spatial frequency for DFWM, A_{21} is the excited state decay rate, D_2 and D_1 are the excited and ground state diffusion coefficients, respectively, and $k_G = 4\pi \sin(\theta/2)/\lambda$ is the grating wave vector formed by the forward pump and probe fields. The relative angular dependence arises from k_G and depends only on the excited state diffusion coefficient D_2 and the decay rate A_{21} . The ground state diffusion coefficient enters only in a constant multiplicative factor that sets the overall magnitude of the induced nonlinear polarization. There is also a similar equation that describes the grating formed by the backward pump and probe fields, but this term is much smaller and its contribution can be neglected.

The fact that only the excited state diffusion determines the relative angular dependence in Eq. (2) can be understood using a simple physical argument. In the steady state, for low input intensities, the excited state grating that has the correct spatial and phase dependence to produce the backwards generated beam is created by the intensity variation produced by the interference of two input beams. This grating is destroyed by both excited state diffusion and decay to the ground state. One can immedi-

ately write the term that gives rise to the four-wave mixing as

$$n_e^G(z) = \frac{N\sigma I^G \sin(k_G z)}{A_{21} + D_2 k_G^2}, \quad (3)$$

where N is the total atomic density, σ is the absorption cross section, I^G is the amplitude of the intensity grating, and the other terms are defined above. This term corresponds to the first term in brackets in Eq. (2). A similar approach can be taken to derive the ground state grating; however, this term is more complicated due to the fact that it has two source terms, namely, depopulation by the writing beams and repopulation from the spatially varying excited state. However, in steady state, the total flux of atoms at any position z must be zero:

$$D_2 \nabla n_2 + D_1 \nabla n_1 = 0. \quad (4)$$

From Eq. (4) it is evident that the strength of the ground state grating will be proportional ($-D_2/D_1$) to the strength of the excited state grating, and it is represented by the second term in brackets in Eq. (2). Thus the relative angular response depends only on the excited state diffusion.

In our experiment, the simple two-level model outlined above needs to be modified due to the fine structure mixing collisions between the $P_{3/2}$ and $P_{1/2}$ states. In this case the two-level model developed above must be expanded to account for mixing to a third level that is not resonant with the input fields [labeled |3⟩ in Fig. 1(b)]. Including this level leads to the same qualitative result that it is only the excited state diffusion that determines the relative angular response. However, the diffusion coefficients and decay rates that are measured are weighted averages of the two fine structure states. For excitation to level |2⟩ the appropriate diffusion coefficient D_2^{eff} and decay rate A_2^{eff} to be used in Eq. (2) are

$$D_2^{\text{eff}} = \frac{D_2(A_{31} + \gamma_{32}) + D_3 \gamma_{23}}{(A_{31} + \gamma_{32}) + \gamma_{23}}, \quad (5)$$

$$A_2^{\text{eff}} = \frac{A_{21}(A_{31} + \gamma_{32}) + A_{31} \gamma_{23}}{(A_{31} + \gamma_{32}) + \gamma_{23}},$$

where D_2 and D_3 are the diffusion coefficients for the levels |2⟩ and |3⟩, γ_{23} and γ_{32} the collisional mixing rates, and A_{21} and A_{31} the radiative decay rates to level |1⟩, respectively. For excitation to level |3⟩, D_3^{eff} and A_3^{eff} are given by Eq. (5) with subscripts 2 and 3 interchanged. For the pressures used in our experiments [14] $\gamma_{23}, \gamma_{32} \gg A_{21}, A_{31}$, so that $D_3^{\text{eff}} \cong D_2^{\text{eff}}$ and $A_3^{\text{eff}} \cong A_2^{\text{eff}}$, and therefore we expect the same relative angular dependence whether we excite to level |2⟩ or to level |3⟩.

Our experimental setup was similar to that described elsewhere [15]. The potassium vapor was contained in Pyrex cells with window separations of 1 mm. The cells were prepared by evacuating them to below 10^{-6} torr, distilling in a small amount of natural potassium metal (94% ^{39}K and 6% ^{41}K), introducing the desired pressure of

Xe, and finally sealing the cell. For this experiment, two cells containing 252 and 485 torr Xe at room temperature were prepared. A frequency-stabilized Ti:sapphire laser was used to generate a probe, a forward pump, and a counterpropagating backward pump beam. All three input beams were vertically polarized, and the generated signal beam had the same polarization. The DFWM signal was observed by using a spatial filter and a polarizer to eliminate stray light. The forward pump-probe angle was varied from 20 to 400 mrad. The forward pump beam was chopped and the signal was measured with a lock-in amplifier. The cells were heated to a temperature of 155 °C, at which the linear intensity attenuation length was approximately equal to the cell length for the $4S_{1/2}-4P_{3/2}$ transition of the lower pressure cell.

All three input beams had nearly the same intensity. For both cells, the total laser intensity was less than the two-level saturation intensity for the $4S_{1/2}-4P_{1/2}$ and $4S_{1/2}-4P_{3/2}$ transitions. This ensured that the use of the third order perturbation expansion [Eq. (2)] for the DFWM signal was valid. The total beam intensities were between 3 and 10 W cm⁻². For both cells, the homogeneous broadening [16] (28 MHz/torr) was much larger than the ³⁹K ground state hyperfine splitting (461 MHz), as well as the Doppler width (900 MHz). For these pressures we estimated that there would be in excess of 100 velocity randomizing collisions during the excited state lifetime, and our diffusion model should be valid. The laser was tuned to the center of the homogeneously broadened transitions, which were red shifted [16] (9.1 MHz/torr), and the DFWM signal was measured as a function of the angle between the two forward-going beams.

Figure 2 shows some data taken with the 252 torr cell. The circles show the measured DFWM signal as a function of the forward pump-probe angle at the conditions described above for the $4S_{1/2}-4P_{1/2}$ transition. The solid line in Fig. 2 is the best fit to the data using the

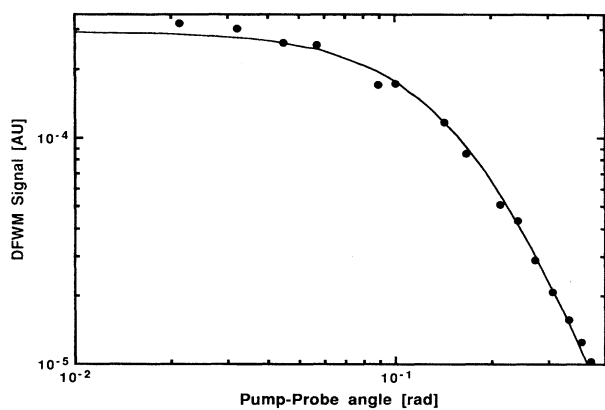


FIG. 2. Experimental DFWM signals from 1.0 mm thick potassium vapor cell with 252 torr Xe. Circles show measured DFWM signals and the solid line is the best fit based on Eq. (2).

predictions based on Eq. (2). The fitting procedure had two free parameters: the diffusion coefficient and the zero angle signal. For the fit we used an excited state lifetime of 27 ns, since collisions mix the two $4P$ states, which have nearly equal lifetimes, and there is little quenching. Data taken using the $4S_{1/2}-4P_{3/2}$ transition had essentially the same angular dependence. For the 485 torr cell the qualitative features were the same except that the angle at which the DFWM signal began to roll off was increased. From analysis of the DFWM signal angular dependence for each cell, we were able to determine the diffusion coefficient at each pressure at the same temperature.

Figure 3 shows the results for the diffusion coefficient plotted vs the reciprocal of the xenon pressure at 155 °C. These data show that there is no variation depending on which transition is utilized. At a constant temperature, the diffusion coefficient is inversely proportional to the pressure, and we have performed a least squares fit of our experimental data to determine the constant of proportionality D , which is the excited state diffusion coefficient at 760 torr. Our results give a value for D at 155 °C of 0.084(4) cm²s⁻¹. Also shown in Fig. 3 is a plot based on calculations from the theoretical predictions for the diffusion cross sections of Hamel *et al.* [17]. Using the potentials of Pascale and Vandeplanque [18], they calculated an excited state diffusion cross section $\sigma_p = 92 \text{ \AA}^2$ at 87 °C, from which we compute $D = 0.103 \text{ cm}^2\text{s}^{-1}$ at 155 °C. Mugglin and Streater [19], using light diffusive pulling, measured the ground state diffusion cross section $\sigma_s = 60(5) \text{ \AA}^2$ and the relative change in the cross section between the ground and excited states

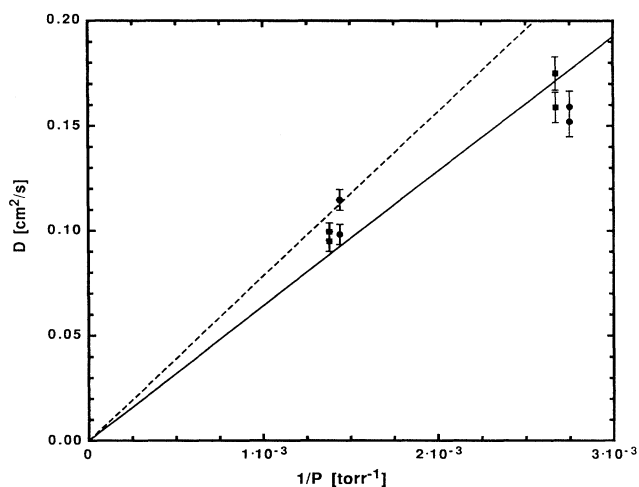


FIG. 3. Plot of measured D at 155 °C vs $1/P$ in torr (pressures at 155 °C). Circles and squares with error bars show experimental results from data similar to Fig. 2, for the transitions $4S_{1/2}-4P_{1/2}$ and $4S_{1/2}-4P_{3/2}$, respectively. The data have been slightly shifted horizontally for clarity. The solid line shows the best fit to our data. The dashed line is calculated from Ref. [17].

$(\sigma_P - \sigma_S)/\sigma_S = 61(5)\%$ at 56 °C, from which we calculated a value of $D = 0.098(12)$ at 155 °C. We have assumed that the diffusion coefficient is proportional to $T^{3/2}$. Our direct measurement of the excited state diffusion coefficient appears to be in approximate agreement with both the theoretical value of Hamel *et al.* and with the indirect measurement of Mugglin and Streater.

In conclusion, we have measured the diffusion coefficient for potassium in xenon gas by using DFWM. Our data are obtained in steady state and do not rely on any time-dependent signal decay to extract the diffusion parameter. We have developed a model that allows us to experimentally determine the diffusion coefficient of the excited P state independently of the diffusion coefficient of the ground state. This new procedure can be extended to measure the diffusion coefficients for any alkali atom in an inert gas. Furthermore, for the cases where there is little excited state mixing, as is the case for Cs and Rb atoms, this technique can readily measure the diffusion coefficients for each P state independently. The increased flat angular response observed using a buffer gas to slow atomic motion through diffusion can also be important for information processing [20], since this will increase the number of pixels in the images that are processed.

We acknowledge partial financial support of this research by the U.S. Army Research Office under Grant No. 30201-PH and the National Science Foundation.

-
- [1] E. A. Mason and T. R. Marrero, *Adv. At. Mol. Phys.* **6**, 155 (1970).
 [2] F. K. Gel'mukhanov and A. M. Shalagin, *Zh. Eksp. Teor. Fiz.* **78**, 1674 (1980) [*Sov. Phys. JETP* **51**, 839 (1980)].

- [3] H. D. C. Werij and J. P. Woerdman, *Phys. Rep.* **169**, 145 (1988).
 [4] F. K. Gel'mukhanov and A. M. Shalagin, *Zh. Eksp. Teor. Fiz.* **77**, 461 (1979) [*Sov. Phys. JETP* **50**, 234 (1979)].
 [5] S. N. Atutov, S. P. Pod'yachev, and A. M. Shalagin, *Zh. Eksp. Teor. Fiz.* **91**, 461 (1986) [*Sov. Phys. JETP* **64**, 244 (1986)].
 [6] S. N. Atutov and A. M. Shalagin, *Pis'ma Astron. Zh.* **14**, 664 (1988) [*Sov. Astron. Lett.* **14**, 284 (1988)].
 [7] D. T. Mugglin, A. D. Streater, S. Balle, and K. Bergmann, *Opt. Commun.* **104**, 165 (1993).
 [8] T. P. Red'ko, *Opt. Spektrosk.* **52**, 769 (1982) [*Opt. Spectrosc. (USSR)* **52**, 461 (1982)].
 [9] R. J. Knize, *Opt. Lett.* **18**, 1606 (1993).
 [10] R. L. Abrams, J. F. Lam, R. C. Lind, D. G. Steel, and P. F. Liao, in *Optical Phase Conjugation*, edited by R. A. Fisher (Academic, New York, 1983), p. 211.
 [11] M. Ducloy and D. Bloch, *J. Phys. (Paris)* **42**, 711 (1981).
 [12] S. M. Wandzura, *Opt. Lett.* **4**, 208 (1979).
 [13] L. M. Humphrey, J. P. Gordon, and P. F. Liao, *Opt. Lett.* **5**, 56 (1980).
 [14] J. Ciurylo and L. Krause, *J. Quant. Spectrosc. Radiat. Transfer* **28**, 457 (1982).
 [15] B. Ai, D. S. Glassner, and R. J. Knize, *Phys. Rev. A* **50**, 3345 (1994).
 [16] N. Allard and J. Kielkopf, *Rev. Mod. Phys.* **54**, 1160 (1982).
 [17] W. A. Hamel, J. E. M. Haverkort, H. G. C. Werij, and J. P. Woerdman, *J. Phys. B* **19**, 4127 (1986).
 [18] J. Pascale and J. Vandeplanque, *J. Chem. Phys.* **60**, 2278 (1974).
 [19] D. T. Mugglin and A. D. Streater, *J. Phys. B* **26**, 689 (1993).
 [20] B. Ai, D. S. Glassner, R. J. Knize, and J. P. Partanen, *Appl. Phys. Lett.* **64**, 951 (1994); I. Biaggio, P. P. Partanen, B. Ai, R. J. Knize, and R. W. Hellwarth, *Nature (London)* **371**, 318 (1994).